Vortex Stretching as a Mechanism for Quantum Kinetic Energy Decay

Robert M. Kerr

Department of Mathematics, University of Warwick, Coventry, United Kingdom CV4 7AL

(Received 21 September 2010; published 1 June 2011)

A pair of perturbed antiparallel quantum vortices, simulated using the three-dimensional Gross-Pitaevskii equations, is shown to be unstable to vortex stretching. This results in kinetic energy $K_{\nabla\psi}$ being converted into interaction energy E_I and eventually local kinetic energy depletion that is similar to energy decay in a classical fluid, even though the governing equations are Hamiltonian and energy conserving. The intermediate stages include the generation of vortex waves, their deepening, multiple reconnections, the emission of vortex rings and phonons, and the creation of an approximately $-5/3$ kinetic energy spectrum at high wave numbers. All of the wave generation and reconnection steps follow from interactions between the two original vortices. A four vortex example is given to demonstrate that some of these steps might be general.

DOI: 10.1103/PhysRevLett.106.224501 PACS numbers: 47.37.+q, 47.27.De, 47.32.C−, 67.25.dk

Background.—Despite the absence of viscosity, experiments have repeatedly shown that superfluids exhibit resistance and depletion of turbulent kinetic energy in a manner similar to the effects of turbulence in a classical fluid [1] with ideal boundary conditions. The superfluid experiments measure the decay of vortex line length, with the first measurements at relatively high temperatures [2] and recent confirmation at lower temperatures. These experiments include ^{3}He for $T < 0.2T_c$ [3], where $T_c \leq 2.2$ mK, and more recent measurements in ^{4}He at $T \leq 0.5$ K [4]. These results imply that the effect could be a property of the ideal, inviscid equations for a pure superfluid or quantum gas, so that coupling to the viscous normal fluid component is not required to get decay.

Why would an inviscid, Hamiltonian system decay in a manner similar to a classical fluid? To compare directly a theory for classical decay based upon the Navier-Stokes equations would be needed, which does not exist. Could large simulations provide the clues? As in the classical case [5,6], a large simulation of a quantum vortex tangle [7] reproduces many experimental properties, including $-5/3$ spectra [8,9]. However, gaining insight has many of the same problems as using observations.

To bridge the gap, this Letter presents initial analysis of the evolution of a single pair of antiparallel quantum vortices that, through a series of identifiable steps, is transformed into a state with most of the observed properties of quantum turbulence. After setting up the problem, analysis shows that after initially stretching, the vortex line length decays along with the local energy. Eventually a $k^{-5/3}$ kinetic energy spectrum forms and distributions of the interaction energy suggest that phonon generation could act as an energy sink. Finally, there are a few results for an initial condition that could be compared to experiments measuring vortex line properties [4,10,11].

Equations and numerics.—The quantum vortices are simulated using the 3D Gross-Pitaevskii equations

$$\frac{1}{i}\frac{\partial}{\partial t}\psi = 0.5\nabla^2\psi + 0.5\psi(1 - |\psi|^2), \tag{1}$$

with background density $\rho_b = 1$. Through the Madelung transformation: $\psi = \sqrt{\rho}\exp(i\phi)$, a velocity is identified as $\boldsymbol{v} = \nabla\phi$ and the density is $\rho = |\psi|^2$. Defects in the wave function ψ are interpreted as infinitesimally thin vortices of constant circulation $\oint \boldsymbol{v}\cdot d\boldsymbol{s} = 2\pi$ The equations conserve the mass $M = \int dV|\psi|^2$ and the Hamiltonian

$$H = K_{\nabla\psi} + E_I \text{ (kinetic + interaction)} \tag{2}$$

where $K_{\nabla\psi} = \frac{1}{2}\int dV\nabla\psi\cdot\nabla\psi^\dagger$, $E_I = \frac{1}{4}\int dV(1-|\psi|^2)^2$, with $\psi^\dagger$ being the complex conjugate of ψ.

Simulations of the Gross-Pitaevskii equations require good numerics, adequate resolution, and smooth boundary conditions. Convergent time advancement is obtained using a 3rd-order Runge-Kutta, semi-implicit spectral algorithm used for other ideal equations [12] where the nonlinear terms are calculated in physical space, then transformed to Fourier space to calculate the linear terms using complex integrating factors. No-flux domain walls are imposed using cosine transforms and serve as an approximation to those of a superfluid in a container and as a means of generating symmetric initial conditions. The constant time step is small enough to obtain convergence consistent with the algorithm.

Initial conditions.—The initial condition for the full periodic domain is shown in Fig. 1(a). The wave function is formed out by superposing vortex cores around the trajectories of lines of $\rho \equiv 0$, then multiplying by complex exponentials, which define the sign of the circulation. In the first case, only one-half of one of the antiparallel pair needs to be given. Its other half and its antiparallel image are automatically behind the no-flux boundaries in y and z. The trajectory chosen for this vortex line is $\boldsymbol{s}(x, y, z) = (\delta_x[2/\cosh([y/\delta_y]^{1.8}) - 1], 1, 0)$ with

$\delta_x = -1.6$ and $\delta_y = 1.25$ in a $L_x \times L_y \times L_z = 8\pi \times 16\pi \times 4\pi$ domain on a $128 \times 512 \times 64$ mesh. The power 1.8 on the normalized position y/δ_y helps to localize the perturbation near the $y = 0$ symmetry plane. Long vortices were used to minimize reflections off the $y = 16\pi$ symmetry plane during the late stages.

To ensure that the initial density went smoothly from zero on the vortex cores to roughly the background density over the distance of the healing length, $|\psi| = \sqrt{\rho} = r^p/\sqrt{r^{2p} + a_0}$ with $p = 2$ and $a_0 = 2$ was chosen. Once the calculation started, the density about the cores profile quickly relaxed to the $p = 1$ theoretical prediction [13]. A new calculation by Rorai starting with $p = 1$ shows cleaner conclusions without changing the overall conclusions about the energetics reported here. This function was applied approximately perpendicular to the trajectory of the vortex lines, and is not perpendicular to the y axis as in past Euler calculations [12], which assisted in minimizing spots of excess $\rho > \rho_b$.

In order to ensure that ψ at the boundaries is sufficiently smooth, up to 23 image vortices from outside the domain were mapped into the computational domain, as opposed to the three image vortices used in earlier work [14]. The final step for obtaining a smooth initial condition uses a $\exp(-\alpha k^4)$ Fourier filter with $\alpha = 0.002$.

Evolution: stretching, reconnection, waves, rings.—To give an overall sense of the evolution, four frames are shown: the initial time and three subsequent stages. Figure 1(b) shows the stretched state just as the first reconnection commences. Vortex stretching modifies the density around the original vortex in several ways. First it deforms the vortex, making it thinner in the x direction. However, because Gross-Pitaevskii does not have singularities, stretching must also remove mass from the interaction region so that the core diameters defined by $\rho \leq \rho_c \approx 0$ can never become infinitely thin. This is distinctly different from the classical Euler equations where singularities are a possibility and cores could become infinitely thin. Figure 1(b) shows the time when this decrease in density has created a density hole between the two vortices and reconnection has begun. As noted before [14], from a Lagrangian perspective, the topologic change associated with reconnection without singularities in the wave function can only occur across locations of zero density. Note the large wave (or kink) at the boundary between the most stretched region and the small vortex waves propagating further out on the vortices.

After reconnection, waves move out from this kink and deepen. These waves are driven by interactions between the vortices, not local induction terms associated with vortex Kelvin waves. The deepening leads to two new reconnections near $|y| = 5$ at $t = 4.5$, which creates the first vortex rings. Then a series of zigzags and dips appear on the $z = 0$ plane. Each of these dips leads to a new reconnection and the creation of yet another vortex ring. Ongoing spectral analysis suggests that for every ring created, there is another spectral cascade step.

The rings then propagate away from the $y = 0$ plane. Figure 2(b) shows a late stage with only a few remaining vortex rings. Note that each successive ring for increasing y has a smaller radius than the previous ring. Because the quantum circulation Γ of each vortex ring is identical, this implies that the propagation velocities $\mathbf{V} \sim \Gamma/R$ and the separation between the rings increases in time and they can freely leave the local system without interfering with one another. The calculation was terminated once the rings began to hit the outer wall.

Stretching diagnostics.—The first attempt to investigate vortex stretching in the Gross-Pitaevski equations used a spectral length similar to the Taylor microscale λ [15]. For the cases here, this length is the order of the vortex diameter and does not grow. A better approach is to mimic experimental measurements of line length that are based upon the scattering of beams of several types by the zero density vortex cores [2–4]. A suitable diagnostic for the length is obtained by counting the number of boxes where $\rho < \rho_c \approx 0$, then dividing by the core cross section for a $p = 1$ profile. Similar algorithms have been used before [16–18] and shown both the growth and decay of vortex

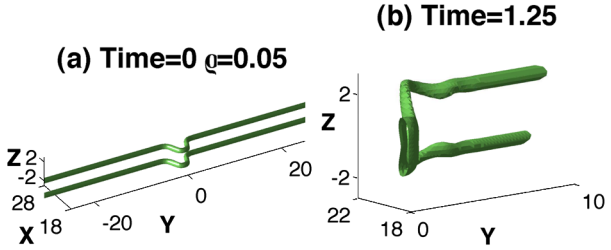

FIG. 1 (color online). Three-dimension isosurfaces with $\rho = 0.05$. Nearly the entire vortices, which extend from $y = -16\pi$ to $y = 16\pi$, are shown in (a). The pair is propagating towards smaller x. In (b), only $y > 0$ is shown to allow us to see into the vortices through the x-z symmetry plane as they are starting to reconnect across the x-y dividing plane. Simultaneously, kinks form on each vortex in y. These kinks are the source of waves that propagate out along the vortices after reconnection.

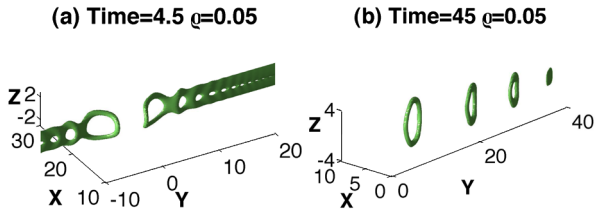

FIG. 2 (color online). (a) $t = 4.5$. After reconnection, the waves deepen until second reconnections occur, allowing vortex rings to separate from the origin vortices. Further incipient reconnections, which lead to the formation of additional vortex rings, can be seen along the vortices. (b) $t = 45$. View showing all the vortex rings for $y > 0$. Multiple vortex rings start separating from the original antiparallel pair starting at $t = 12$ and propagate to larger y. By $t = 45$ some have left the system.

lines. Using $\rho_c = 0.1$, Fig. 3 quantifies the stretching seen up to $t \approx 4.5$ and the subsequent decay of line length.

Decay relations.—With a direct simulation, an experimentally observed property such as the decay of vortex line length can be directly compared to the different components of energy and used to test whether the interpretation of the decay of line length as a measure of energy decay is valid and can be compared with theories.

A possible relationship between line length and kinetic energy is obtained through squaring the line length, which provides an estimate for the effective enstrophy Z or mean square vorticity. As demonstrated in a simulation of classical, homogeneous isotropic turbulence in a periodic box [1], because the enstrophy Z is related to the dissipation of kinetic energy by $\epsilon = (d/dt)K = \nu Z$, if the vortex line length is defined as $L = \int ds \approx \sqrt{Z}$ and is observed to decay as $L \sim t^{-3/2}$, then $Z \sim t^{-3}$ and the kinetic energy decays as $K \sim t^{-2}$. This decay law is never seen experimentally, as all classical experiments have boundary layers.

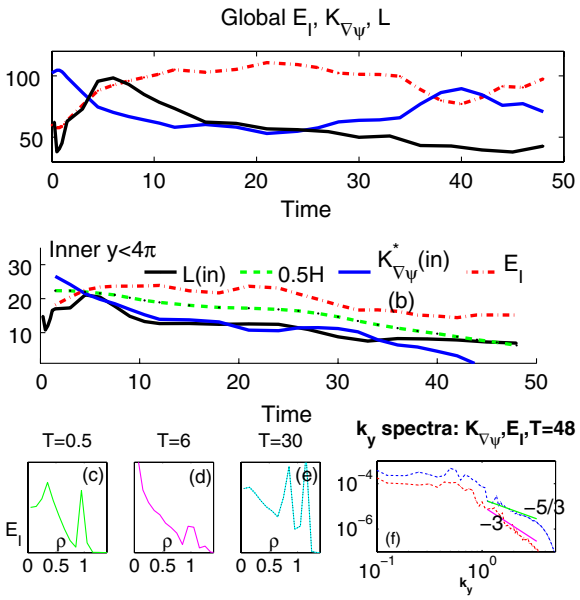

FIG. 3 (color online). Estimates of the line length compared to changes in the interaction and kinetic energies. (a) Analysis over the full domain. There is strong E_I and vortex line growth (L) for $0.5 < t < 6$. For $6 < t < 25$ both $K_{\nabla\psi}$ and L decrease. For $T > 30$ the global kinetic energy $K_{\nabla\psi}$ grows again. This is associated with the accumulation of energy for $y > 4\pi$. (b) Only the first y quadrant, the original interaction region. Here too, the initial length and E_I grow at the expense of $K_{\nabla\psi}$. Later $K_{\nabla\psi}$, half the total Hamiltonian $0.5H$ and L decrease. (c)–(e) Distributions of the E_I with respect to density at $t = 0.5$, 6, 30 to show how energy appears to flow from $K_{\nabla\psi}$ to E_I to waves. Spectra: (f) by $t = 48$, $K_{\nabla\psi}(k_y)$ has an enhancement high wave number regime compared to E_I. Spectra in the other directions have similar trends but are less distinct. For comparison k^{-3} and $k^{-5/3}$ lines are drawn to demonstrate this effect, which could be indicating some type of downscale energy cascade in $K_{\nabla\psi}$.

Without a normal fluid, the current consensus is that energy can be removed in a quantum fluid only by the nonideal boundaries. The outstanding question is to explain how the energy gets there. Three mechanisms have been proposed: (i) quantum vortex lines reconnect to form vortex rings, which then propagate out [19]; (ii) linear waves, or phonons, are generated internally and propagate out; (iii) waves on vortices could cascade to small scales and their energy be radiated as phonons [20].

After a brief adjustment from the initial condition, completed by $t = 0.5$, the two primary stages shown in Figs. 3(a) and 3(b) are as follows. (I) E_I increases, $K_{\nabla\psi}$ decreases, and L grows until the second reconnection near $t = 4.5$ occurs, which is when the first and largest vortex ring separates off, as illustrated by Fig. 2. (II) Thereafter, as multiple vortex rings and phonons are being generated, the local $K_{\nabla\psi}$ decreases and L decays.

The depletion in line length with time is not continuous, it occurs in steps, making it impossible to compare this single series of events with power law decay. Each step can be associated with specific events, either reconnections or rings leaving the local domain.

Distributions and line length.—To understand the different stages, subplots Figs. 3(c)–3(e) show distributions of the interaction energy E_I (2) with respect to density at 3 times. The $t = 0.5$ distribution in Fig. 3(c) demonstrates that initially E_I has a maximum near $\rho = 1$.

Figure 3(d) shows that at $t = 6$, when stretching is greatest, there has been a dramatic growth in E_I, with most of the growth for $\rho \approx 0$. This implies a large growth in the number of points with $\rho \approx 0$. Note that the increases in E_I for $t \leq 20$ are compensated for by a strong decrease in the global kinetic energy in Fig. 3(a).

Immediately after $t = 6$, L begins to decrease dramatically while the kinetic energy $K_{\nabla\psi}$ continues to decay, which is compensated for by a continuing increase in the interaction energy E_I. At the end of this stage, there is a growth in large values of E_I on either side of $\rho = 1$, shown by the distribution at $t = 30$—around, not at, because for $\rho = 1$, $E_I \equiv 0$. This would be consistent with visualizations of waves being emitted from colliding vortices [18,21].

The decrease in the global kinetic energy does not persist. Eventually interaction energy is converted back into kinetic energy, possibly due to oscillations between $K_{\nabla\psi}$ and E_I in the released phonons. Similar oscillations were observed in Gross-Pitaevskii calculations with a symmetric Taylor-Green initial condition [15]. This would not persist in a real experimental device because the waves would be absorbed by the nonideal boundaries.

To mimic what decay in a real flow might look like, especially experiments that generate tangles far from boundaries [4], Fig. 3(b) shows the growth, then decay, of the line length in the first y quadrant ($0 \leq y \leq 4\pi$) with rescaled kinetic energy, showing that the local region exhibits kinetic energy depletion in the final phase as the vortex rings leave this region.

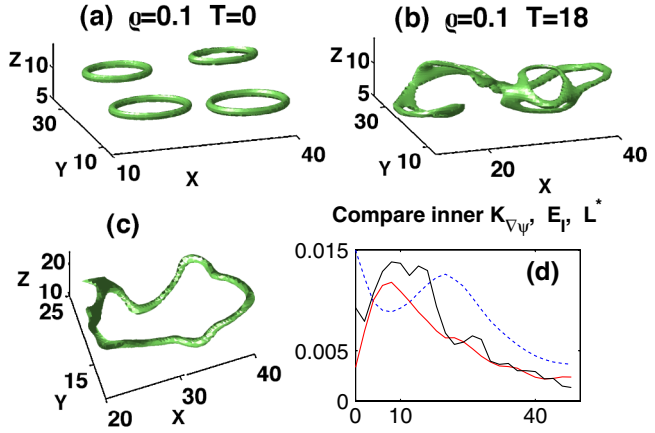

FIG. 4 (color online). Four colliding rings, the entangled state generated, the final relaxed state, and the time dependence of the kinetic and interaction energies plus a measure of line length in the inner region that contained the original vortices. In this case the measure of line length, the volume where $\rho < 0.1$, tracks the interaction energy E_I more closely than the kinetic energy.

Spectral cascade.—Is there a cascade to small scales? Figure 3(f) shows spectra for the final time $t = 48$. $E_I(k_y)$ and $K_{\nabla\psi}(k_y)$ are shown because they are directly related to conservation of energy and because they do not have artificial high wave number regimes created by the singularities in the vortex cores. In the first state of spectral development, until the first ring separates off at $t = 4.5$, high wave number spectra are roughly k^{-3} in all directions for both E_I and $K_{\nabla\psi}$. This is similar to spectra in Euler calculations [12]. After $t = 4.5$, $K_{\nabla\psi}(k)$ gradually increases at higher wave numbers, that is smaller scales, but not $E_I(k)$. The spectra shown at $t = 48$ represent the end of this process with $E_I(k_y) \sim k^{-3}$, while $K_{\nabla\psi}(k_y) \sim k^{-5/3}$. The transfer of $K_{\nabla\psi}$ to small scales is the significant observation, not the exact power laws. Preliminary analysis of the spectral interactions suggests a type of dual cascade, with $K_{\nabla\psi}$ having a forwards cascade while E_I cascades to large scales through nonlocal wave number interactions.

Colliding rings.—How much of the scenario portrayed here has been seen before? To address this question, initial conditions similar to earlier work have been simulated [14,17,21]. Of these cases, a four ring case in Fig. 4 provides the best qualitative support for how generic the role of stretching and reconnection seen here are. Figure 4 shows that (A) as the vortex rings become entangled in Fig. 4(b), kinetic energy decreases sharply while interaction energy and line length increase, and (B) as the tangle disintegrates and small rings are released in Fig. 4(c), all local quantities decay. Note: In this four vortex case, line length is closely tied to E_I, which decays more rapidly than $K_{\nabla\psi}$.

In both of these cases and a previous four ring case [17], there are multiple reconnections and strong intervortex interactions. Recalculation and analysis of orthogonal and two ring initial conditions [14,18,21], generate only one or two reconnections, not the scenario here.

Summary.—A long-standing question in classical turbulence is whether the energy cascade is mostly statistical, or originates with the interaction of fluid structures. No matter how special or nonclassical, even a single case that started with a simple vortical configuration and then generated a cascade could provide new insight. Such an initial condition could then be adapted to classical reconnection and turbulence calculations to determine whether similar dynamics and stages can form. The results here suggest how to start a search for similar classical events that would begin with vortex stretching, then form a tangle followed by multiple reconnections, and finally lead to the creation of small scale dissipative structures.

Discussions and communications with C. Barenghi, M. E. Fisher, A. Golov, D. D. Holm, D. P. Lathrop, T. Lipniacki, C. Rorai, B. Svistunov, and W. F. Vinen are appreciated. Partial support for this work was provided by the Leverhulme Foundation Grant No. F/00 215/AC and the EU-COST on Aerosols and Particles in Turbulence. Computational support was provided by the Warwick Centre for Scientific Computing.

[1] R. M. Kerr, Ph.D. thesis, Coop. Thesis No. 64, Cornell University and NCAR, 1981; digitized copy at http://nldr.library.ucar.edu/repository/osgc/OSGC-000-000-001-855. This result was first noted by S. Patterson.
[2] M. R. Smith *et al.*, Phys. Rev. Lett. **71**, 2583 (1993).
[3] D. I. Bradley *et al.*, Phys. Rev. Lett. **96**, 035301 (2006).
[4] P. M. Walmsley and A. I. Golov, Phys. Rev. Lett. **100**, 245301 (2008).
[5] R. M. Kerr, J. Fluid Mech. **153**, 31 (1985).
[6] Y. Kaneda *et al.*, Phys. Fluids **15**, L21 (2003).
[7] J. Yepez *et al.*, Phys. Rev. Lett. **103**, 084501 (2009).
[8] J. Maurer and P. Tabeling, Europhys. Lett. **43**, 29 (1998).
[9] P.-E. Roche *et al.*, Europhys. Lett. **77**, 66002 (2007).
[10] K. W. Schwarz and R. J. Donnelly, Phys. Rev. Lett. **17**, 1088 (1966).
[11] G. P. Bewley *et al.*, Proc. Natl. Acad. Sci. U.S.A. **105**, 13 707 (2008).
[12] M. D. Bustamante and R. M. Kerr, Physica (Amsterdam) **237D**, 1912 (2008).
[13] N. G. Berloff, J. Phys. A **37**, 1617 (2004).
[14] J. Koplik and H. Levine, Phys. Rev. Lett. **71**, 1375 (1993).
[15] C. Nore, M. Abid, and M. E. Brachet, Phys. Rev. Lett. **78**, 3896 (1997); Phys. Fluids **9**, 2644 (1997).
[16] S. Z. Alamri, A. J. Youd, and C. F. Barenghi, Phys. Rev. Lett. **101**, 215302 (2008).
[17] M. Leadbeater *et al.*, Phys. Rev. A **67**, 015601 (2003).
[18] N. G. Berloff, Phys. Rev. A **69**, 053601 (2004).
[19] R. P. Feynman, Prog. Low Temp. Phys. **1**, 17 (1955).
[20] B. Kozik and B. Svistunov, Phys. Rev. Lett. **92**, 035301 (2004).
[21] M. Leadbeater *et al.*, Phys. Rev. Lett. **86**, 1410 (2001).